Electronic Supplementary Material (ESI) for Sustainable Energy & Fuels.

Supporting information

Advanced electrocatalyst for efficient synthesis of ammonia based on chemically coupled NiS@MoS_2 heterostructured nanospheres

Shoushuang Huang [a], Chunyan Gao [a], Peijun Xin [a], Haitao Wang [a], Xiao Liu [a], Ye Wu [a], Qingquan He [a], Yong Jiang [a], Zhangjun Hu [*, a, b], Zhiwen Chen[*, a]

[a] School of Environmental and Chemical Engineering, Shanghai University, Shanghai, 200444, China

[b] Division of Molecular Surface Physics & Nanoscience, Department of Physics, Chemistry and Biology, Linköping University, Linköping 58183, Sweden

Corresponding Author:

E-mail: zwchen@shu.edu.cn

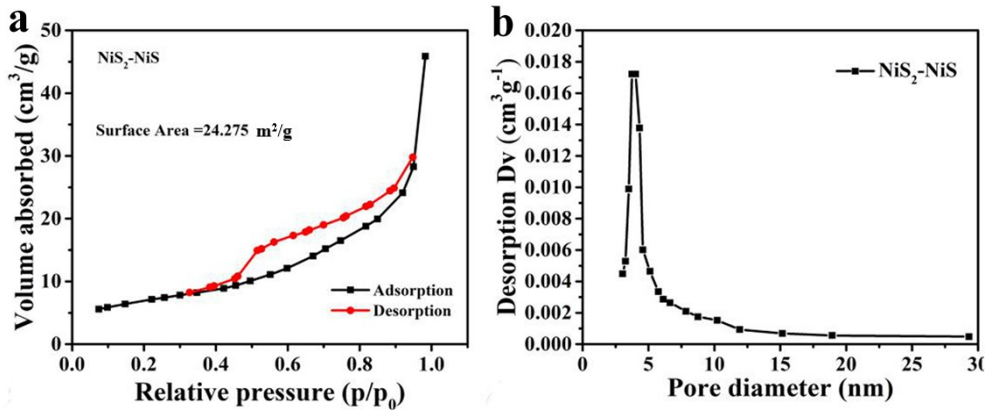

Fig. S1. (a) Nitrogen adsorption/desorption isotherms. (b) Pore diameter distribution curve of NiS_2-NiS nanospheres.

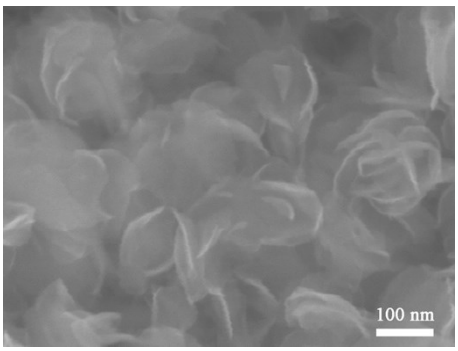

Fig. S2. SEM image of the as-synthesized pure MoS_2 product.

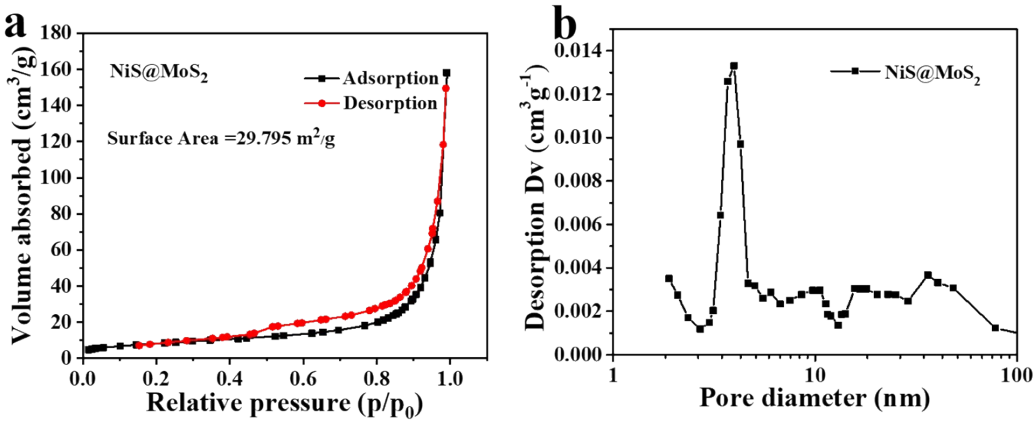

Fig. S3. (a) Nitrogen adsorption/desorption isotherms. (b) Pore diameter distribution curve of NiS@MoS_2 nanocomposites.

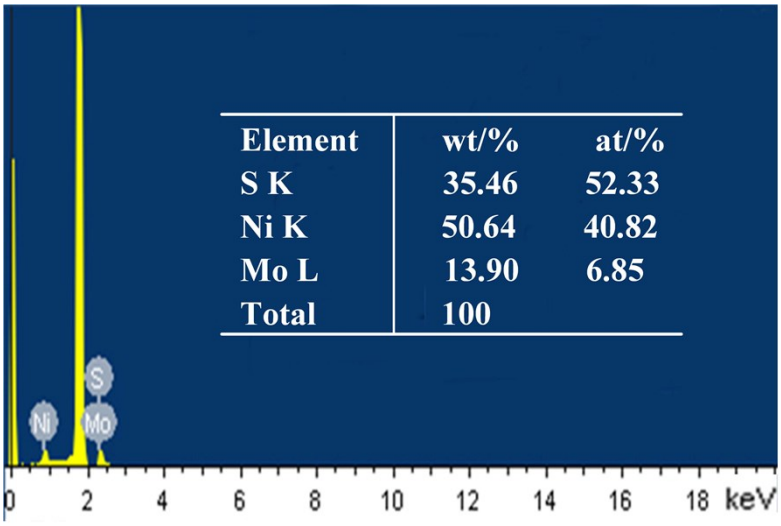

Fig. S4. The energy-dispersive X-ray spectroscopy (EDX) of the as-synthesized NiS@MoS_2 heterostructures.

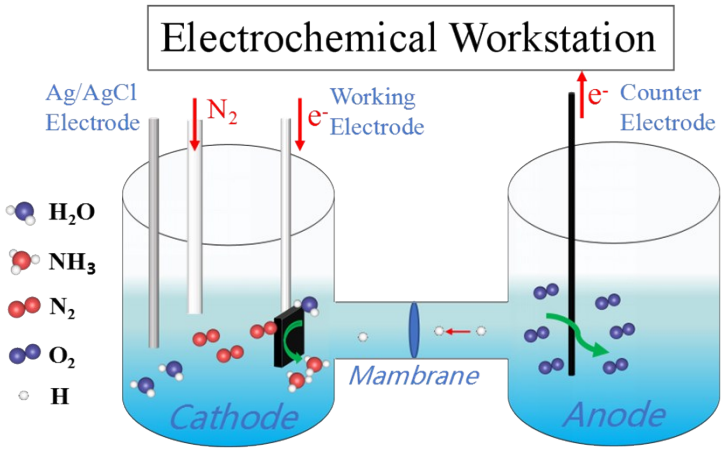

Cathode: $N_2+6H_2O+6e^- \longrightarrow 2NH_3+6OH^-$

Anode: $6OH^- \longrightarrow 1.5O_2+6e^-+3H_2O$

Total: $N_2+3H_2O \longrightarrow 2NH_3+1.5O_2$

Fig. S5. Schematic illustration of the NRR process.

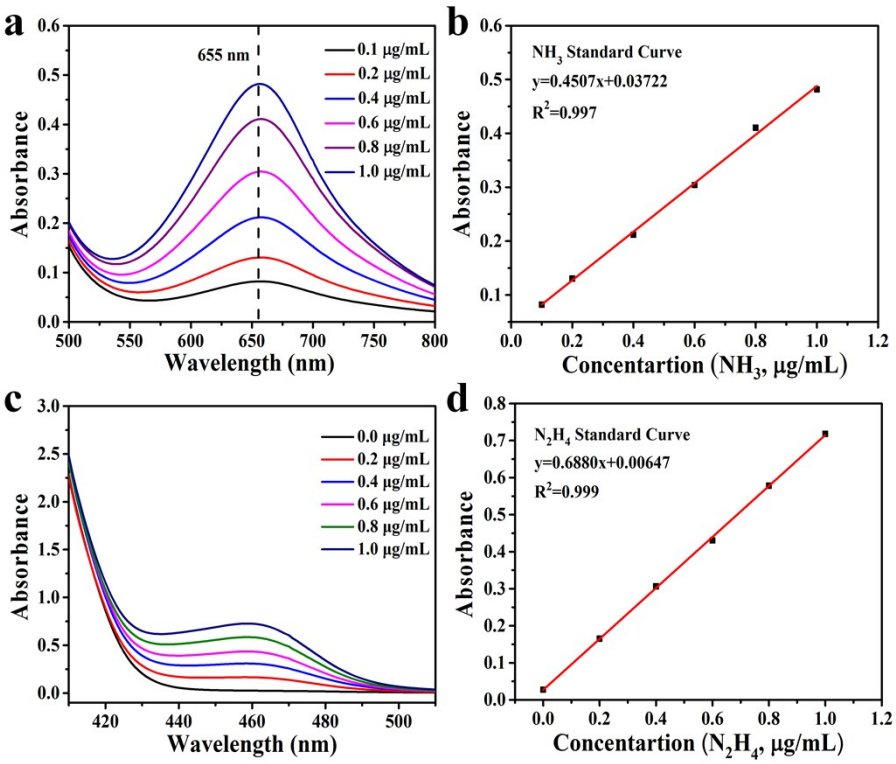

Fig. S6. (a) Absorbance spectra of indophenol blue in NH_4^+ solutions at various concentrations. (b) Linear correlation of the absorbance intensity to NH_4^+ concentration. (c) UV-vis curves of $N_2H_4 \cdot H_2O$ after incubated for 10 min at room temperature. (d) Calibration curve used for calculation of N_2H_4 concentration.

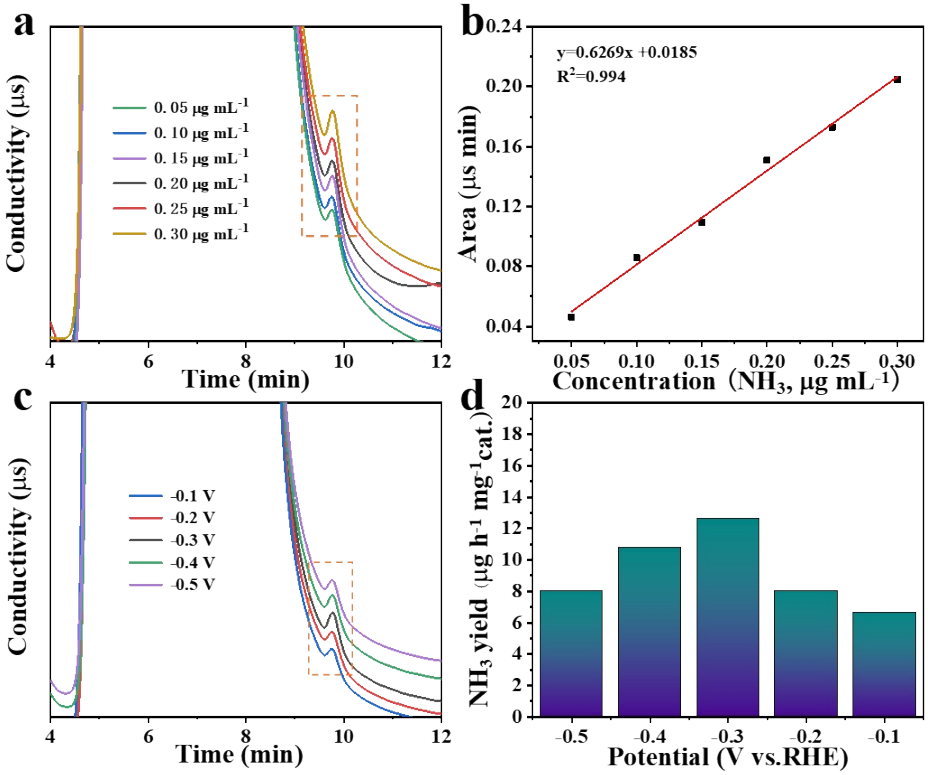

Fig. S7. (a) Ion chromatogram of NH_4Cl with different concentrations in 0.1 M Na_2SO_4 and (b) corresponding standard curve. (c) Ion chromatogram for the electrolytes at a series of potentials after electrolysis for 2 h. (d) NH_3 yield of NiS@MoS_2 at corresponding potentials.

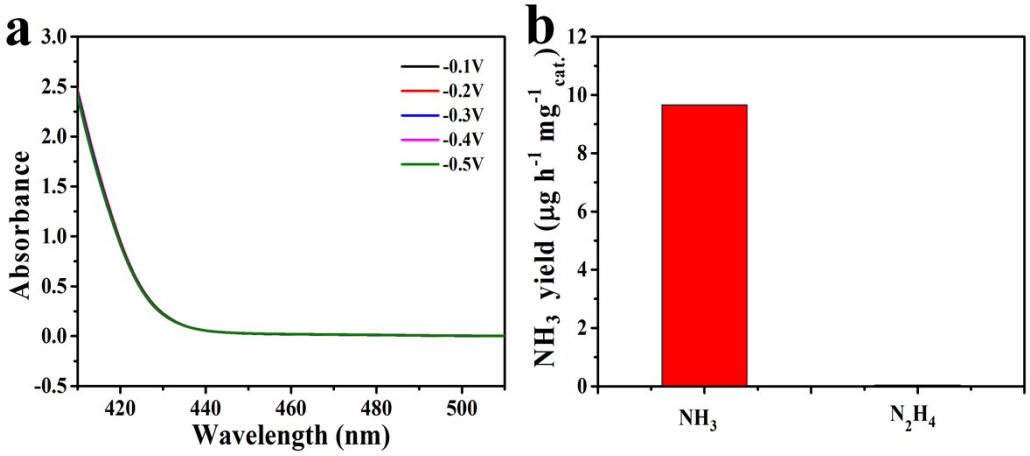

Fig. S8. (a) UV-vis absorption spectra of the electrolytes stained by the Watt and Chrisp method after potentiostatic tests. (b) The yield rate for ammonia and hydrazine generated during electrochemical NRR at –0.3 V vs. RHE.

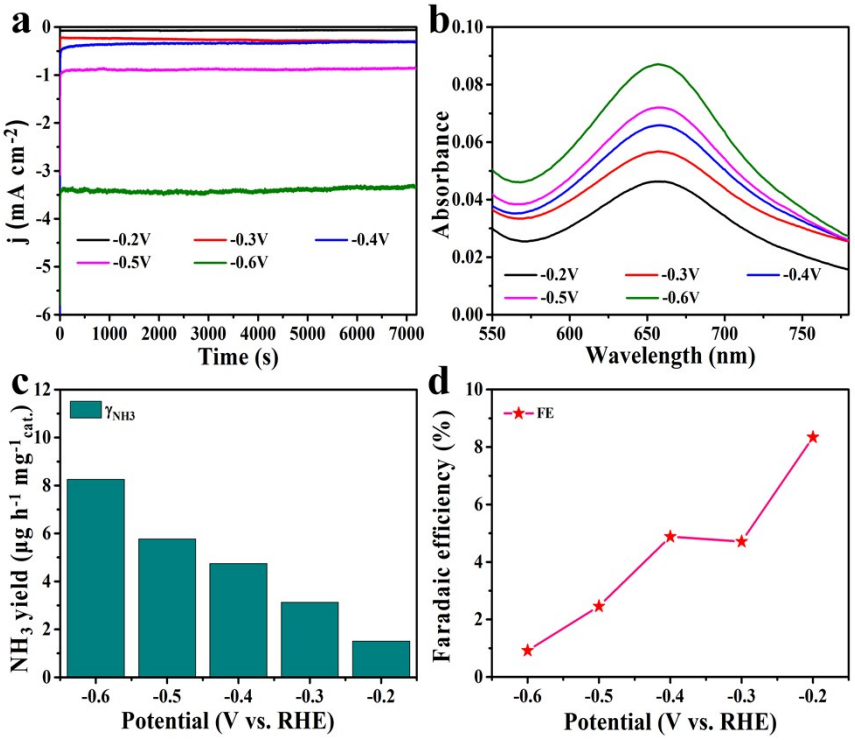

Fig. S9. NRR electrocatalysis of MoS_2. (a) CA tests for 2 h with MoS_2 electrode at various potentials from –0.6 to –0.2 V vs. RHE. (b) Corresponding UV-vis spectra of electrolytes colored with indophenol indicator. (c) Ammonia yield rates at various potentials. (d) Faradaic efficiencies at various potentials.

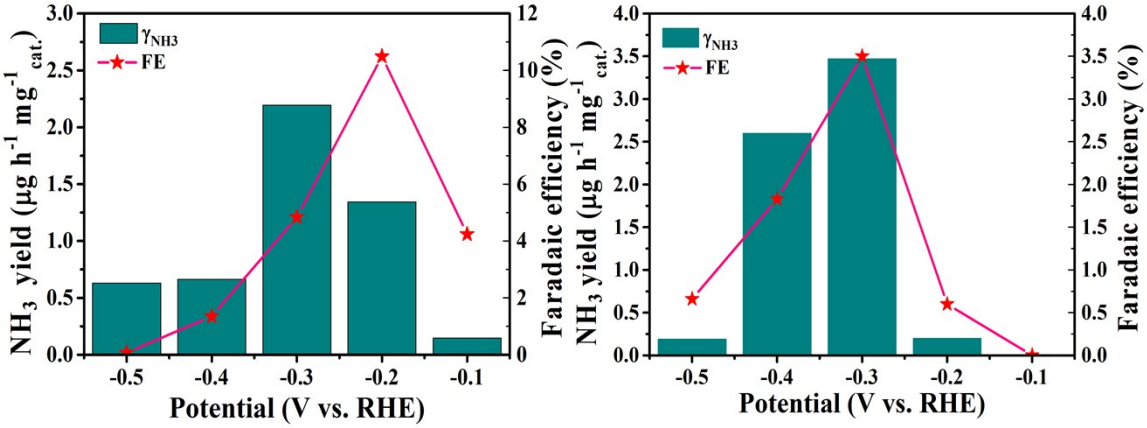

Fig. S10. NH_3 yields and Faradaic efficiencies for γ-NiOOH/NiS_x (a) and NiS_2-NiS (b) at a series of potentials for 2 h.

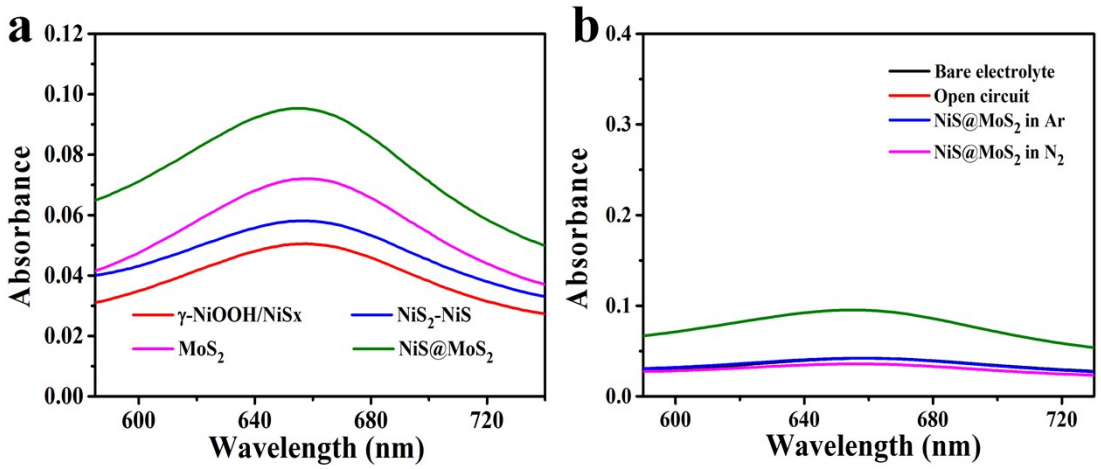

Fig. S11. (a) Comparison of catalytic performances of various electrocatalysts at -0.3 V vs. RHE. (b) UV-vis absorption spectra of the electrolytes stained with an indophenol indicator after potentiostatic tests under different conditions.

Table S1. Comparison of the electrocatalytic N_2 reduction performance for NiS@MoS_2 with other aqueous-based NRR electrocatalysts under ambient conditions.

Catalyst	**Electrolyte**	**NH_3 yield**	**FE (%)**	**Ref.**
NiS@MoS_2	0.1 M Na_2SO_4	9.66 μg h^{-1}·mg^{-1}_{cat}	14.8	**This work**
Pd/C	0.1 M PBS	4.5 μg h^{-1}·mg^{-1}_{cat}	8.2	[1]
γ-Fe_2O_3	0.1 M KOH	0.212 μg h^{-1}·mg^{-1}_{cat}	1.9	[2]
$Pd_{0.2}Cu_{0.8}$/rGO	0.1 M KOH	2.8 μg h^{-1}·mg^{-1}_{cat}	4.5	[3]
α-Au/CeOx-RGO	0.1 M HCl	8.31 μg h^{-1}·mg^{-1}_{cat}	10.1	[4]
Au nanorods	0.1 M KOH	6.042 μg h^{-1}·mg^{-1}_{cat}	4	[5]
Fe_2O_3-CNT	$KHCO_3$	0.22 μg h^{-1} cm^{-2}	0.15	[6]
Pd-Co/CuO	0.1 M KOH	10.04 μg h^{-1}·mg^{-1}_{cat}	2.16	[7]
Fe/Fe_3O_4	0.1 M PBS	0.19 μg h^{-1} cm^{-2}	8.19	[8]
Mo nanofilm	0.01 M H_2SO_4	1.89 μg h^{-1} cm^{-2}	0.72	[9]
PEBCD/C	0.5 M Li_2SO_4	1.58 μg h^{-1} cm^{-2}	2.85	[10]

References

[1] J. Wang, L. Yu, L. Hu, G. Chen, H.L. Xin, X.F. Feng, Nat. Commun. 9 (2018).

[2] J. Kong, A. Lim, C. Yoon, J.H. Jang, H.C. Ham, J. Han, S. Nam, D. Kim, Y.-E. Sung, J. Choi, H.S. Park, ACS Sustainable Chem. Eng., 5 (2017) 10986-10995.

[3] M.-M. Shi, D. Bao, S.-J. Li, B.-R. Wulan, J.-M. Yan, Q. Jiang, Adv. Energy Mater. 8 (2018).

[4] S.-J. Li, D. Bao, M.-M. Shi, B.-R. Wulan, J.-M. Yan, Q. Jiang, Adv. Mater. 29 (2017).

[5] D. Bao, Q. Zhang, F.-L. Meng, H.-X. Zhong, M.-M. Shi, Y. Zhang, J.-M. Yan, Q. Jiang, X.-B. Zhang, Adv. Mater. 29 (2017).

[6] S. Chen, S. Perathoner, C. Ampelli, C. Mebrahtu, D. Su, G. Centi, Angew. Chem., Int. Ed. 56 (2017) 2699-2703.

[7] W. Fu, Y. Cao, Q. Feng, W.R. Smith, P. Dong, M. Ye, J. Shen, Nanoscale 11 (2019) 1379-1385.

[8] L. Hu, A. Khaniya, J. Wang, G. Chen, W.E. Kaden, X. Feng, ACS Catal. 8 (2018) 9312-9319.

[9] D. Yang, T. Chen, Z. Wang, J. Mater. Chem. A 5 (2017) 18967-18971.

[10] G.-F. Chen, X.R. Cao, S.Q. Wu, X.Y. Zeng, L.-X. Ding, M. Zhu, H.H. Wang, J. Am. Chem. Soc. 139 (2017) 9771-9774.